Nuclear Instruments and Methods in Physics Research A 678 (2012) 39–47

Contents lists available at SciVerse ScienceDirect

Nuclear Instruments and Methods in Physics Research A

journal homepage: www.elsevier.com/locate/nima

Effects of errors in velocity tilt on maximum longitudinal compression during neutralized drift compression of intense beam pulses: II. Analysis of experimental data of the Neutralized Drift Compression eXperiment-I (NDCX-I)

Scott Massidda [a], Igor D. Kaganovich [a,*], Edward A. Startsev [a], Ronald C. Davidson [a], Steven M. Lidia [b], Peter Seidl [b], Alex Friedman [c]

[a] Plasma Physics Laboratory, Princeton University, Princeton, NJ 08543, USA
[b] Lawrence Berkeley National Laboratory, 1 Cyclotron Road, Berkeley, CA 94720, USA
[c] Lawrence Livermore National Laboratory, 7000 East Avenue, Livermore, CA 94550, USA

ARTICLE INFO

Article history:
Received 21 October 2011
Received in revised form
8 March 2012
Accepted 13 March 2012
Available online 21 March 2012

Keywords:
Neutralized drift compression

ABSTRACT

Neutralized drift compression offers an effective means for particle beam focusing and current amplification with applications to heavy ion fusion. In the Neutralized Drift Compression eXperiment-I (NDCX-I), a non-relativistic ion beam pulse is passed through an inductive bunching module that produces a longitudinal velocity modulation. Due to the applied velocity tilt, the beam pulse compresses during neutralized drift. The ion beam pulse can be compressed by a factor of more than 100; however, errors in the velocity modulation affect the compression ratio in complex ways. We have performed a study of how the longitudinal compression of a typical NDCX-I ion beam pulse is affected by the initial errors in the acquired velocity modulation. Without any voltage errors, an ideal compression is limited only by the initial energy spread of the ion beam, ΔE_b. In the presence of large voltage errors, $\delta U \gg \Delta E_b$, the maximum compression ratio is found to be inversely proportional to the geometric mean of the relative error in velocity modulation and the relative intrinsic energy spread of the beam ions. Although small parts of a beam pulse can achieve high local values of compression ratio, the acquired velocity errors cause these parts to compress at different times, limiting the overall compression of the ion beam pulse.

Published by Elsevier B.V.

1. Introduction

Longitudinal bunch compression is a standard technique used to increase the beam intensity in various accelerators [1]. Previous longitudinal drift compression analysis has studied the effects of intrinsic beam momentum spread, plasma, and solenoidal final focus conditions on compression [1,2]. Much focus has also gone towards space-charge neutralization [1,3,4]. The kinematics of neutralized compression drift is well developed [5]. Here, we focus on the most important effect that limits the beam compression—the errors in the voltage in the bunching module. This paper is a companion paper of Ref. [6], which analyzes the general properties of the effects of errors on longitudinal compression. Here, we apply the formalism developed in Ref. [6] to the analysis of the experimental data of the Neutralized Drift Compression eXperiment-I (NDCX-I).

In neutralized drift compression the applied velocity tilt, Δv_b, slows down the head of the ion beam pulse and speeds up the tail of the pulse so that the entire beam pulse compresses at a later time, t_f, at the target plane, l_f. The velocity tilt is produced by an induction bunching module. Ideally, the voltage profile of the induction bunching module is designed such that the entire beam pulse arrives at one location at the focusing time. The corresponding beam velocity profile is called an ideal tilt. In this case, the effects associated with a small, non-removable intrinsic energy spread, ΔE_b, would limit the compression. Ref. [2] suggested several possible mechanisms for increasing the energy spread, including two-dimensional effects in the diode and collective effects due to the beam space charge. A detailed numerical study of both effects was performed; the study made it clear that neither mechanism leads to significant energy spread [6,7]. However, the longitudinal non-removable energy spread can be caused by transit time effects in the bunching module. Due to the time-dependant nature of the bunching module, the beam energy acquired in the gap is not exactly equal to the potential drop inside the gap. There are corrections due to transit time effects in the

* Corresponding author. Tel.: +1 609 243 3277; fax: +1 609 243 2418.
E-mail address: ikaganov@pppl.gov (I.D. Kaganovich).

0168-9002/$ - see front matter Published by Elsevier B.V.
http://dx.doi.org/10.1016/j.nima.2012.03.008

bunching module. For a gap of a few centimeters, the beam requires 25–30 ns to cross through the gap, i.e., about 10–20% of the modulating waveform duration time (about 300 ns). Therefore, transit time effects can be important. This correction to the beam energy was calculated in Ref. [6]:

$$\Delta E_b(\tau,r) = eV(\tau)\left[1 - \frac{eV'(\tau)\gamma_w R_w}{2E_b^{in} v_b^{in}}\left(1 - \frac{r^2}{2b^2}\right)\right]. \tag{1}$$

Here, $V(\tau)$ is the voltage on the bunching module as a function of time τ, R_w is the pipe radius, $b \approx 2 \times 0.73 R_w/\sqrt{\pi} \approx 0.84 R_w$ and $\gamma_w \approx 0.33$. A small radial variation of the electric field in the bunching module leads to corrections to the energy change acquired in the gap. A small variation of the beam energy as a function of radius given by Eq. (1) is of order $0.1(eV)^2 r_b{}^2/E_b^{in} t_p v_b R_w$ and can be a very small fraction of the bunching voltage $\sim (eV)/1000$. However, this energy spread is not removed during neutralized ballistic focus (in contrast to the space charge beam self-potential, which is removed during the transition to the neutralized region [6]) and can give rise to effective "thermal" energy spread in induction bunching modules. For example, $\Delta E_b(r)$ is of order 100 eV for NDCX-I parameters. Another mechanism can be voltage drift on the ion source diode. For the NDCX-I experiment the measurements of the energy spread give $\Delta E_b < 170$ eV [8]. Therefore, below, *we assume that the beam pulse has non-removable energy or effective "thermal" velocity spread, which is not associated with ion source temperature but rather due to imperfections of the accelerator system.* However, voltage errors in the induction bunching module are of the order 1 kV and thus are primarily responsible for the limitation of longitudinal compression.

Due to voltage errors and corresponding errors in the applied velocity tilt, δv_b, parts of the ion beam pulse arrive at different times. The compressed beam pulse width at the target chamber is of order $l_f = \delta v_b t_f$, where t_f is the drift time. This gives a pulse duration of order $\Delta v_b t_f / v_b^{in}$, where v_b^{in} is the original velocity of the beam determined by the initial beam energy. During the drift, the head and tail of the pulse of duration, t_p, approach the target nearly simultaneously, i.e., the pulse length is $l_p \equiv v_b^{in} t_p = \Delta v_b t_f$. Correspondingly, the compression ratio is of order [6]

$$C \sim \frac{l_p}{l_f} = \frac{v_b^{in} t_p}{\delta v_b t_f} = \frac{\Delta v_b}{\delta v_b}. \tag{2}$$

From Eq. (2), it is evident that the portion of the beam pulse with the smallest errors contributes most to the compression. If the velocity errors are much smaller for the fraction of the pulse, δt_p, then the compression ratio is given by

$$C \sim \frac{\Delta v_b \delta t_p}{\delta v_b t_p}. \tag{3}$$

If beam velocity errors become so small that they are comparable to the "thermal" spread, then the compression ratio is limited by the velocity describing energy spread, v_T, i.e.

$$C \sim \frac{\Delta v_b \delta t_p}{v_T t_p}. \tag{4}$$

Correspondingly, the maximum compression ratio is determined by the condition that the largest fraction of the pulse compresses with the smallest velocity errors. For example, for a model of fast changing errors on a scale t_{er} that is small compared to the initial pulse width in the form $\Delta v_b = \Delta v_b \sin(t/t_{er})$, the fraction of the pulse that compresses is given by $\delta t_p \approx t_{er}(4v_T/\delta v_b)^{1/2}$ [6] and

$$C \sim \frac{2\Delta v_b}{(v_T \Delta v_b)^{1/2}} \frac{t_{er}}{t_p}. \tag{5}$$

Therefore, the maximum compression ratio is a function of both the intrinsic velocity spread and the velocity errors in the bunching module.

Using previously derived analytical formulas from Ref. [6] for calculating the compression ratio of a particular velocity tilt, together with particle-in-cell simulations, data from NDCX-I experiments have been analyzed using a fully kinetic treatment. It was found that the compression ratio is a function of both errors in the applied velocity tilt and the initial energy spread of the beam pulse.

This paper is organized as follows: Section II provides the basic equations; Section III applies the results to the NDCX-I experiment; and Section IV summarizes the conclusions.

2. Basic equations

In this section we provide a summary of the analytical description of the longitudinal compression ratio, explained in greater detail in Ref. [6]. First, we describe the compression ratio without taking thermal effects into account. The beam acquires velocity, $v_b(\tau)$, in the induction bunching module, where τ denotes the time at which the beam interacts with the bunching module. The head of the pulse acquires velocity $v_{b0} \equiv v_b(0)$. The parameter τ can be viewed as a marker for a particular part of the ion beam pulse, $0 \le \tau \le t_p$, where t_p is the duration of the pulse that is expected to compress. The trajectory of a beam pulse at time t, interacting with the bunching module at time τ, is given by

$$z_b(t,\tau) = v_b(\tau)(t-\tau) \tag{6}$$

which represents the acquired velocity multiplied by the drift time. An ideal trajectory has all parts of the beam pulse arriving at the target plane at the same time, $z_b(t_f,\tau) = l_f$, for all τ. This requires the *ideal* velocity tilt,

$$v_b^i(\tau) = v_{b0} t_f/(t_f - \tau). \tag{7}$$

Note that $v_{b0} t_f = l_f$, and by varying the parameters v_{b0} and t_f, different ideal velocity tilts can be chosen that would allow the beam to compress at a certain location l_f or time t_f.

The longitudinal density is given by the ratio of the initial and final separation of the beam slices: $n_b(\tau,t) = n_b^{in}|dz_0/dz_b|$, where n_b^{in} is the initial beam ion line density before the bunching module. Substituting for $z_b(t,\tau)$ from Eq. (6) gives

$$n_b(\tau,t) = \frac{n_b^{in} v_b^{in}}{|v_b(\tau) - (t-\tau) dv_b(\tau)/d\tau|}. \tag{8}$$

A convenient way to characterize the compression of the pulse is to introduce the time to focus [6], $t_s(\tau)$, when different parts of the ion beam pulse compress, or when neighboring slices of the beam arrive at the same position. In Lagrangian coordinates, this corresponds to a singularity in the beam line density profile given by Eq. (8), which occurs at time

$$t_s(\tau) = \frac{v_b(\tau)}{dv_b(\tau)/d\tau} + \tau. \tag{9}$$

An ideal velocity tilt will have $t_s(\tau) = t_f$ for all τ, which implies that all parts of the pulse compress at the same time.

Another convenient way to examine the beam dynamics is by plotting the beam pulse in phase-space coordinates, (z, v_z). As the beam moves through phase space, the velocity tilt that represents the beam moves with it, becoming a vertical line when the beam is compressed. Vertical lines in phase space correspond to peaks in compression. To remove the singularity in Eq. (8), the compression ratio has to be calculated by taking thermal effects into account. The compression ratio is determined by counting the number of particles that arrive at a certain location z, at time t [6], i.e.

$$n_b(z,t) = \int_{-\infty}^{t} v_b^{in}\, d\tau \int_{-\infty}^{\infty} dv f(v) \Delta(z - z_b(t,\tau) - vt) \tag{10}$$

where $f(v)$ is the initial velocity distribution function of the beam ions. This formula allows the compression ratio to be calculated for any applied velocity tilt. The maximum compression ratio for an ideal tilt is obtained by comparing the initial pulse length, $t_p v_b^{in}$, to the final spread, limited only by the intrinsic Maxwellian velocity distribution of the initial pulse with mean velocity v_T [6], i.e.

$$C^i{}_{max} = \frac{t_p v_b^{in}}{\sqrt{\pi} v_T t_f}. \tag{11}$$

For example, for NDCX-I parameters, the ion beam energy is 300 keV, and $T_{bz} \simeq 0.3\,\mathrm{eV}$, $v_T/v_b^{in} \approx 10^{-3}$; and for a velocity tilt, $\Delta v_b/v_b^{in} = t_p/t_f = 0.15$, $t_f \sim 3\,\mu\mathrm{s}$, $t_p \sim 0.45\,\mu\mathrm{s}$, and Eq. (11) gives $t_f \sim 3\,\mu\mathrm{s}$, $v_b t_p \sim 45\,\mathrm{cm}$, $\sqrt{\pi} v_T t_f \sim 0.4\,\mathrm{cm}$ and $C_{max} = 110$. For the case of smaller $T_{bz} \simeq 0.05\,\mathrm{eV}$, we obtain $C_{max} = 255$.

This can be compared to the compression ratio of a pulse with voltage errors, δU. Here, the compression ratio is shown to be a weak function of intrinsic "thermal" spread, v_T, and the relative error in applied energy $\delta U/E_b$ [6] is given by

$$C^b{}_{max} \approx \frac{\tau_\gamma}{t_f} \left(\frac{v_{b0}}{v_T \Delta U/E_b} \right)^{1/2}. \tag{12}$$

Here, τ_γ is the characteristic temporal scale for a change in the velocity errors. For NDCX-I, $\Delta U/E_b \sim 1/300$, and $\tau_\gamma \sim 300\,\mathrm{ns}$. This gives a maximum compression ratio of about 60.

Note that a thermal equilibrium distribution in beam energy corresponds to a Gaussian distribution in energy spread, $\Delta E_b \approx M(v - v_b) v_b$, with

$$f_M(\Delta E) = \frac{1}{\sqrt{2\pi T_z/M}} \exp\left(-\frac{(\Delta E)^2}{4 E_b T_z} \right).$$

Correspondingly, the standard deviation for the energy spread is $2\sqrt{E_b T_z}$; the average dispersion of the energy spread is $\sqrt{\langle (\Delta E)^2 \rangle} = \sqrt{2 E_b T_z}$; and the full width at half maximum of the energy spread is $2\sqrt{E_b T_z \ln(2)}$. For example, for $T_{bz} \simeq 0.1\,\mathrm{eV}$ and $E_b = 300$ keV, the energy spread dispersion is 245 eV and the standard deviation is 347 eV.

Based on the results of the experimental study in Ref. [8], the upper bound of the beam energy spread is 100 eV (see Ref. [6] Section II c 2 for a more complete discussion). Consequently, it is assumed in the following analysis that $T_{bz} = T_i = 0.05$–0.1 eV, and that the value is determined by the ion source temperature.

3. Analysis of effects of voltage errors on longitudinal compression ratio for NDCX-I experiments

The NDCX-I experimental configuration is well described in several publications [9–12]. In these experiments, a potassium ion beam with energy of about 300 keV passes through an induction bunching module and then drifts through a neutralized drift section about 3 m in length. As a result, part of the beam (about 500 ns) is compressed to a few ns. Experimentally-achieved compression ratios range from 50 to 90, depending on the beam energy and the target location. We have performed a detailed analysis of the longitudinal compression ratio for the voltage pulse waveform shown in Fig. 1, and a drift section with length 286.8 cm. The data is taken from Ref. [13]. We have found that the maximum compression ratio can increase from 60 to 90 for optimal beam energy, in agreement with the experimental data. We have also analyzed other data sets and found results similar to the data shown in Fig. 1.

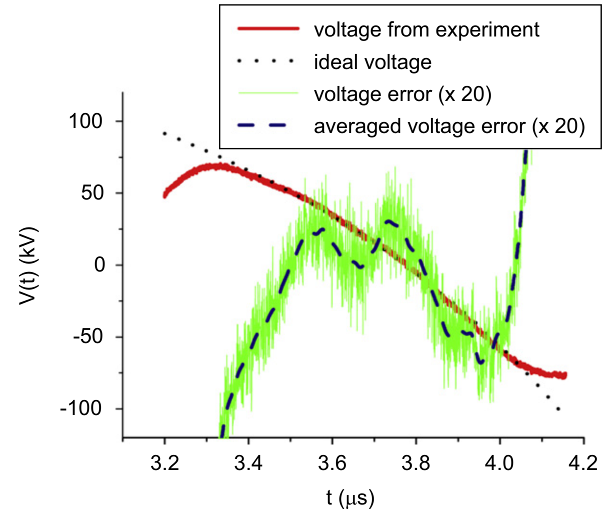

Fig. 1. Plots of experimental voltage waveform of the NDCX-I induction bunching module [13] as a function of time and the ideal voltage waveform needed to compress the beam pulse at the target plane for beam energy 270 keV (dotted curve). Also shown is the error in the experimental voltage as compared with the ideal voltage pulse and the Gaussian-weighted averaged value of the error with a 20 ns time window performed to remove high-frequency noise.

As evident from Fig. 1, the experimental voltage waveform is close to the ideal voltage waveform pulse starting at $t_0 = 3.48\,\mu\mathrm{s}$ and ending at $t_1 = 4.07\,\mu\mathrm{s}$ for a total duration of $t_p = 0.59\,\mu\mathrm{s}$. Therefore, this part of the beam pulse is expected to compress. At the beginning of the pulse, the beam head is decelerated from 270 kV to 210 kV at $t_0 = 3.48\,\mu\mathrm{s}$, and accelerated from 270 kV to 348 kV at the end of the pulse, at $t_1 = 4.07\,\mu\mathrm{s}$. Note that the voltage polarity shown in Fig. 1 is such that a positive voltage corresponds to beam deceleration. The ideal voltage waveform is given by

$$U(t) = \frac{M}{2} \left\{ [v_b^i(t)]^2 - v_b^2(t_0) \right\} \tag{13}$$

where $v_b^i(\tau) = v_{b0} t_f/(t_f - \tau)$ and $\tau = (t - t_0)$. Here, we have assumed the thin-gap approximation, in which the drift time through the gap can be neglected. Corrections to the thin-gap approximation are discussed in Ref. [6], and are mostly reduced to averaging the voltage errors over the time scale of the drift through the gap:

$$V(\tau) \to \int_{-\infty}^{\infty} \frac{V(\tau')}{\triangle\tau\sqrt{\pi}} \exp\left[-\frac{(\tau' - \tau)^2}{\triangle\tau^2} \right] d\tau'.$$

The transit time, $\Delta\tau$, is $b/v_b^{in} = 30\,\mathrm{ns}$, where $b \approx 2 \times 0.73 R_w/\sqrt{\pi}$ and R_w is the pipe radius [6].

3.1. Choosing parameters for an ideal voltage pulse

The applied voltage errors are at the level of several percent. Therefore, the ideal voltage waveform parameters (t_f and v_{b0}, or E_{b0}, the beam energy at the start of the beam pulse) can also be chosen within several percent accuracy, as evident in Fig. 2. For example, the choice of $t_f = 2.83\,\mu\mathrm{s}$ and $E_{b0} = 210$ keV corresponds to a beam pulse compressed at $v_{b0} t_f = 288.3$ cm, in the limit of ideal compression ratio without any errors. This compression plane is slightly behind the target positioned at 286.8 cm. Choosing $t_f = 2.679\,\mu\mathrm{s}$ and $E_{b0} = 217$ keV corresponds to the ideal beam pulse compressed at the target location, $v_{b0} t_f = 286.8$ cm. Similarly, the choice of $t_f = 2.77\,\mu\mathrm{s}$ and $E_{b0} = 208$ keV corresponds to a compression plane located at $v_{b0} t_f = 281$ cm, just before the target plane. The compressed beam profiles at different locations are shown in Fig. 3.

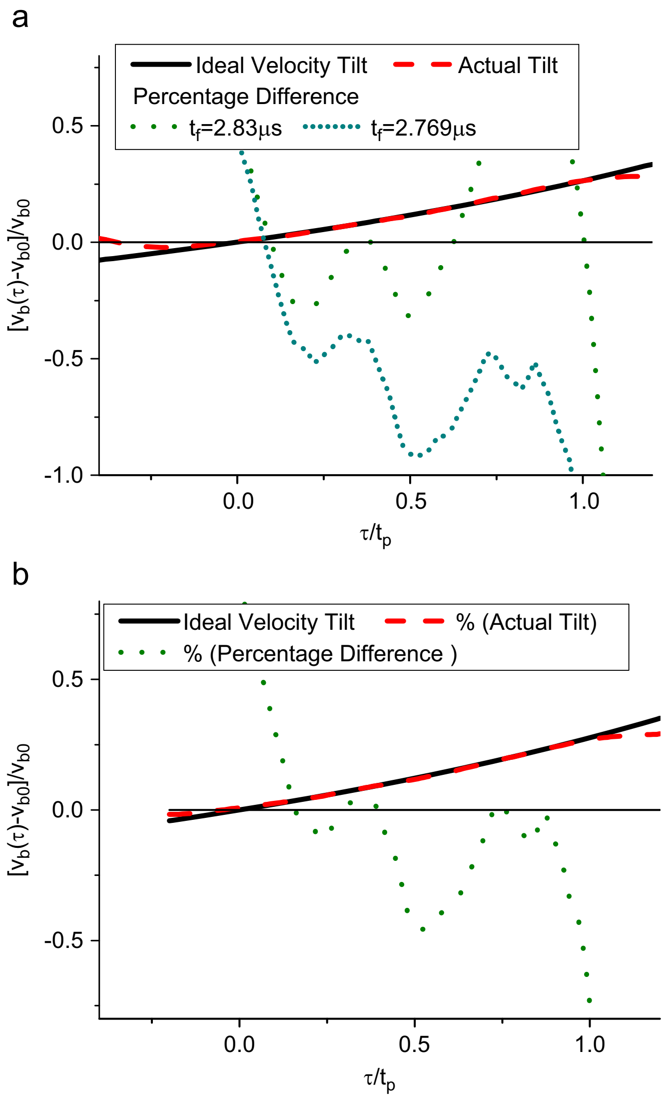

Fig. 2. Normalized beam velocity tilt $\Delta v_b/v_{b0}$ is plotted as a function of normalized time τ/t_p in the tilt core for the voltage pulse waveform shown in Fig. 1. The solid curve shows the ideal velocity tilt given by Eq. [7] for (a) t_f =2.83 μs, E_{b0}=210 keV and t_f =2.679 μs, E_{b0}=217 keV, and (b) t_f =2.725 μs, E_{b0}=208 keV. The dashed and dotted curves show the experimental velocity tilt and the value of the error in percent, respectively.

3.2. *Spread of compression locations due to fast changing errors in the voltage pulse*

From Fig. 3 it is evident that the beam pulse compresses significantly at different positions, which are spread over large distances relative to the target plane. This behavior can be explained by plotting the times when different parts of the beam pulse compress according to Eq. (9), as shown in Fig. 4. The compression time, or the time when neighboring slices of the beam arrive at the same position, depends on the time derivative of the voltage waveform. Therefore, small but fast-changing errors result in large variations of the compression time of different parts of the beam pulse. That is, 1% errors in the beam velocity tilt can result in 10–20% variations of the compression time, as evident from Fig. 4. A zoomed-in plot of the compression ratio is shown in Fig. 5. It is evident from Fig. 5 that the compressed pulse foot width is of order 10 ns due to the errors, but the compressed pulse full width at half maximum can be reduced to a few ns for optimum beam energy [compare Fig. 5(a) and (b)]. Indeed, if there is an error in the beam velocity,

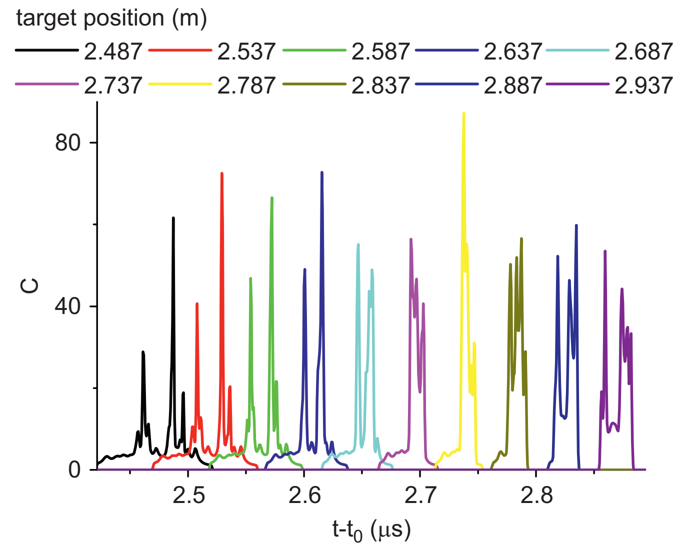

Fig. 3. Simulated compressed pulse waveform at 10 different target locations from z=248.7 cm to 293.7 cm plotted as a function of drift time after the beam pulse passes through the induction bunching module for the voltage waveform shown in Fig. 1. The beam energy is 270 keV, and the longitudinal temperature, T_z, is 0.05 eV.

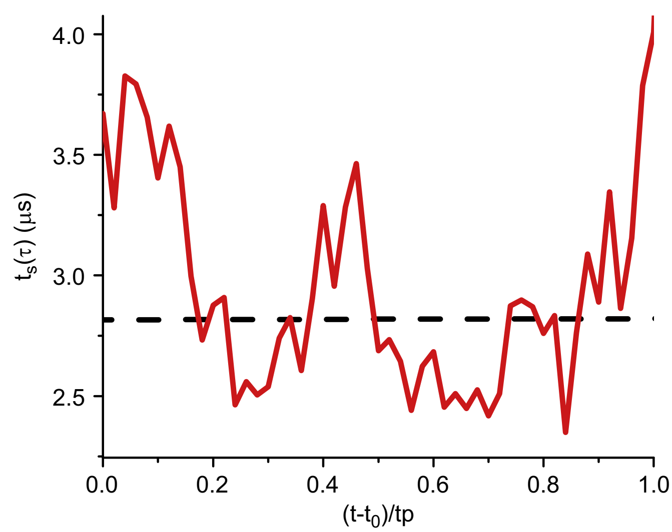

Fig. 4. Time $t_s(\tau)$ when neighboring slices of the beam arrive at the same position is plotted as a function of normalized time, $(t-t_0)/t_p$, where $\tau = t-t_0$. The solid (red) curve corresponds to the experimental voltage waveform shown in Fig. 1, and the dashed (black) curve corresponds to the ideal voltage pulse. (For interpretation of the references to color in this figure legend, the reader is referred to the web version of this article.)

δv_b, due to voltage errors, the beam pulse width at the target plane is $\delta v_b t_f$.

Correspondingly, the beam pulse duration at the target plane due to voltage errors of 1 kV for a 300 keV beam is $\Delta v_b t_f/v_{b0} \sim 2.8\,\mu s/300 \approx 10\,\text{ns}$. For the optimum beam energy or target location, the voltage errors are a factor of three smaller for this part of the beam pulse (see Fig. 2), and the corresponding compressed pulse width is reduced from 10 ns to 3 ns [compare Fig. 5(a) and (b) or Fig. 3, for z_t=2.737 m and z_t=2.787 m].

3.3. *Scaling of the compression ratio with reduced voltage errors*

If the voltage errors are reduced, the compressed beam pulse width is also reduced and the compression ratio is increased.

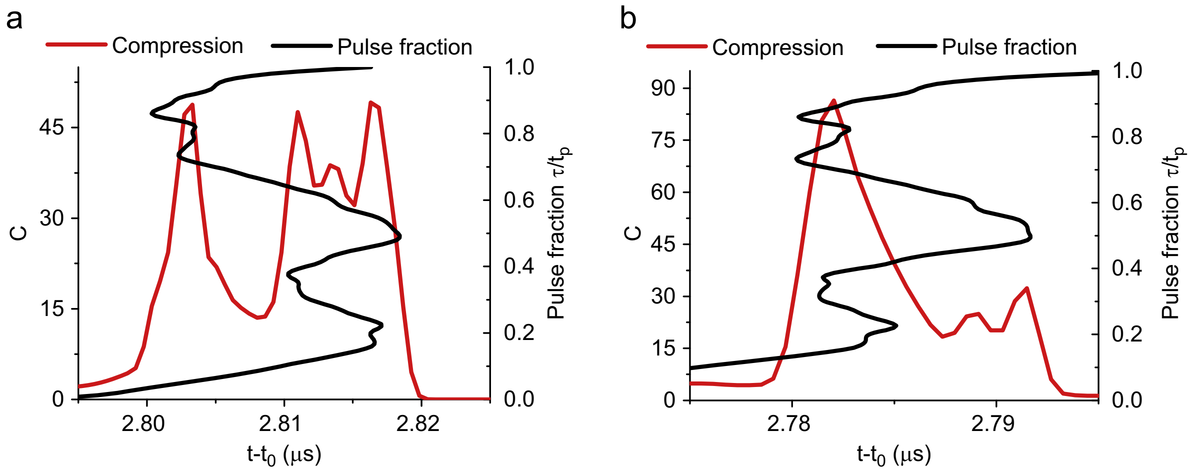

Fig. 5. Simulated compressed pulse waveform at the target location $z=286.8$ cm is plotted as a function of the drift time for the voltage waveform shown in Fig. 1. The beam energy is (a) 270 keV and (b) 276 keV, and the longitudinal temperature is $T_z=0.05$ eV.

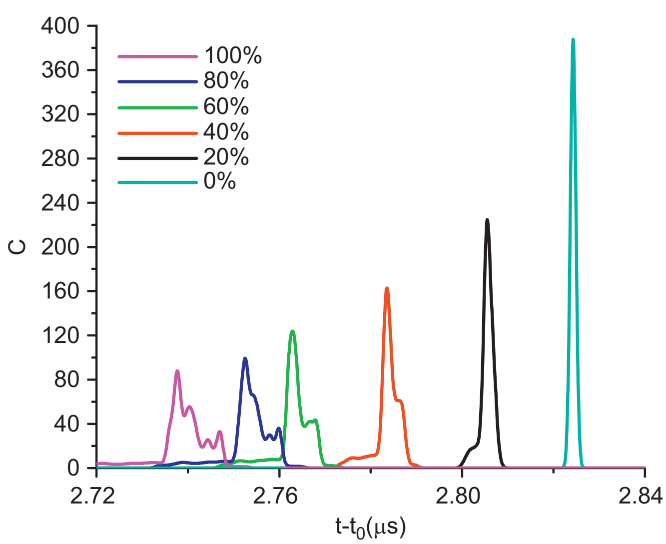

Fig. 6. Simulated compressed pulse waveform at optimal target locations (100% error, $z=279$ cm; 80%, 280 cm; 60%, 281 cm; 40%, 284 cm; 20%, 286 cm; 0%, 288 cm) is plotted for reduced voltage errors as a function of drift time for the voltage waveform shown in Fig. 1. The beam energy is 270 keV, and the longitudinal temperature is $T_z=0.05$ eV.

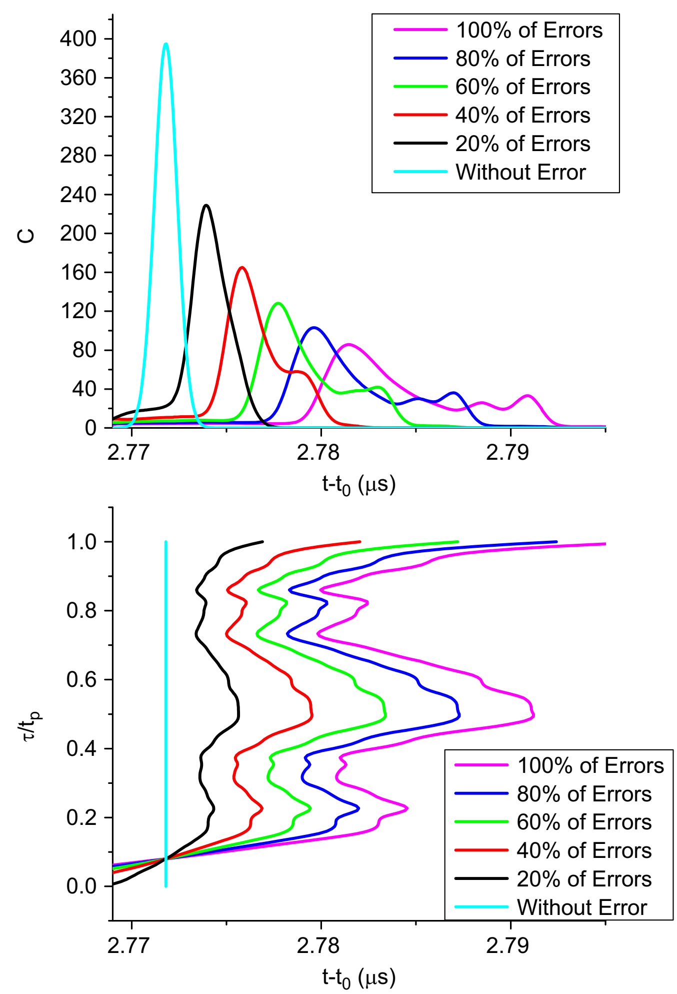

Fig. 7. Simulated compressed pulse waveform (top) and original pulse Lagrangian coordinate τ (bottom) at the target location, $z=286.8$, for reduced voltage errors are plotted as a function of drift time for the voltage waveform shown in Fig. 1. The longitudinal temperature is $T_z=0.05$ eV.

The effect of reduced errors is shown in Figs. 6 and 7. Reducing the errors by a factor of five only increases the compression ratio by a factor of two (compare black and magenta curves in Figs. 6 and 7). This is in agreement with Eq. (12), which shows that the compression ratio is inversely proportional to the square root of the velocity errors and the intrinsic "thermal" spread, as shown in Fig. 8.

3.4. Observation of multiple peaks and optimization of compressed beam pulse by varying the beam energy

If the voltage profile is smooth, the beam compresses at an optimal location, and then two peaks appear, corresponding to compression in the head and tail [see Ref. [6]]. This is similar to compression in klystrons; however, in the induction bunching module with many separate pulsed elements, the fast-changing voltage errors lead to the formation of multiple peaks. The optimal compression corresponds to the case when a few major peaks overlap, or equivalently, when voltage errors are minimized for a few portions of the beam pulse. We demonstrate this by analyzing the compression with an improved voltage pulse on NDCX-I compared to the one shown in Fig. 1.

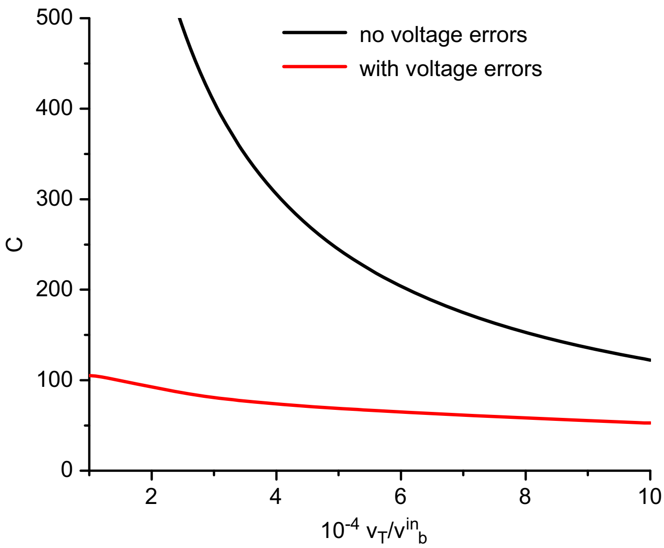

Fig. 8. Simulated compression ratio at the target location $z=2.77$ cm and drift time t–$t_0=2.73$ ms is plotted as a function of the normalized thermal velocity, v_T/v_b^{in}, for the voltage waveform shown in Fig. 1. The beam energy is 270 keV, and the longitudinal temperature, $T_z=0.05$ eV, corresponds to $v_T/v_b^{in}=3\times10^{-4}$. The black curve corresponds to the ideal velocity tilt with no errors, and the compression ratio as a function of the thermal spread is given by Eq. (11).

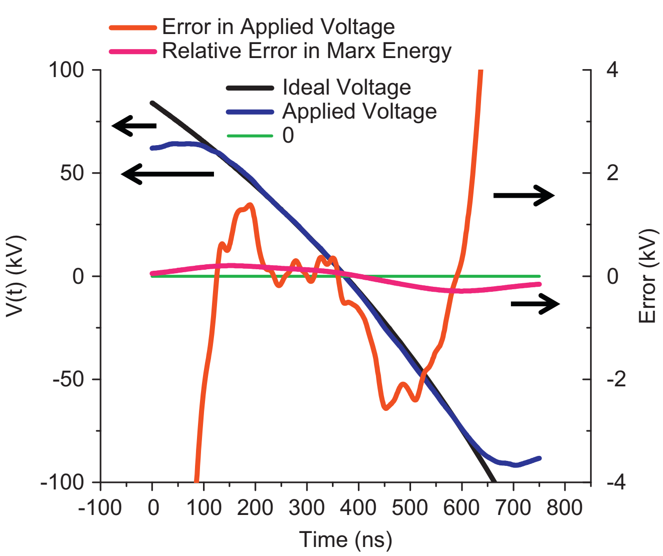

Fig. 9. Plots of improved experimental voltage waveform of the NDCX-I induction bunching module as a function of time, and the ideal voltage waveform needed to compress the beam pulse at the target plane for beam energy 319 keV (black curve). Also shown is the Gaussian-weighted averaged value of the error (with a 21 ns time window) in the experimental voltage as compared with the ideal voltage pulse. Finally, the relative error in beam energy delivered by the Marx generator is shown to be small compared with applied voltage error.

NDCX-I improvements in the induction bunching module reduced voltage errors; however, the errors are still of order ~1 keV. There is a portion of the pulse near the middle where the errors are low, and this allows more of the pulse to compress at the focusing time, thereby increasing the compression ratio and reducing the pulse length. This can be compared with the middle of the previous waveform, which did not compress with the rest of the beam pulse, leaving a significant portion of the pulse uncompressed.

The intrinsic "thermal" spread length is the mean drift length of the ions due to the intrinsic thermal energy spread of the beam pulse, $\pm v_T t_f$. Fig. 10 shows that much of the pulse does not

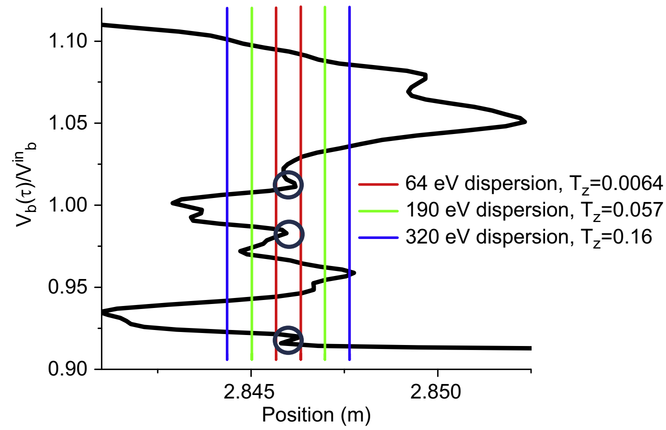

Fig. 10. Phase space plot of the pulse with different mean intrinsic energy spreads, $E_{b0}=322$ keV and $t_f=2.628$. The target location is 2.846 m. The parallel red lines indicate a mean particle drift due to an intrinsic energy spread of 64 eV; the parallel green lines correspond to a spread of 190 eV; and the parallel blue lines correspond to 320 eV. The three circles represent regions of high density. (For interpretation of the references to color in this figure legend, the reader is referred to the web version of this article.)

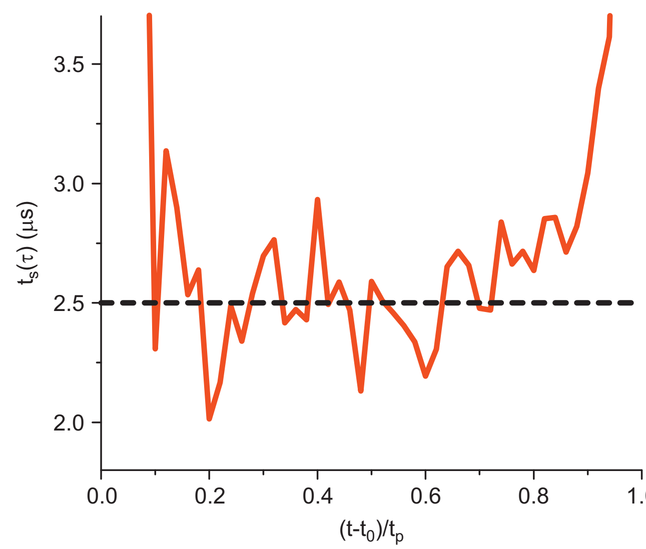

Fig. 11. Time $t_s(\tau)$ when neighboring slices of the beam arrive at the same position is plotted as a function of normalized time $(t-t_0)/t_p$, where $\tau=t-t_0$. The solid (red) curve corresponds to the experimental voltage waveform shown in Fig. 9, and the dashed (black) curve corresponds to the ideal voltage pulse. (For interpretation of the references to color in this figure legend, the reader is referred to the web version of this article.)

compress within a distance $\pm v_T t_f$, even for the time of optimal compression. Errors need to be reduced by a factor of 10 to be on the same order as the energy spread, ~100 eV. Figs. 11 and 12 show that the pulse represented by the waveform in Fig. 9 compresses for a wide range of locations near the target plane. The time to focus, t_s, in Fig. 11 can be compared to the drift time, t–t_0, in Fig. 12.

The compression ratio profile in NDCX-I is measured using a Fast Faraday Cup (FFC), which has a time-scale response of 1 ns [13]. During the initial tuning process of the experiment, multiple peaks are often observed before the final calibrations are made, as shown in Fig. 13. The energy of the beam, E_{b0}, needs to be tuned to ensure that the beam focuses at the target plane. However, compression is still observed even before the final tuning, indicating that the beam compresses over a range of target locations.

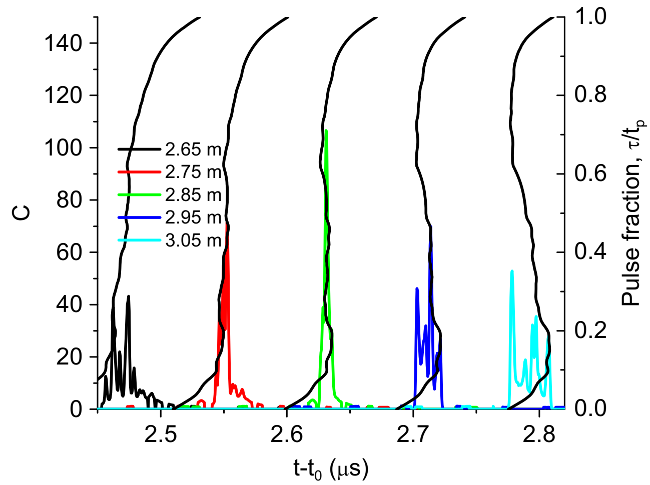

Fig. 12. Simulated compressed pulse waveform at five different target locations, from $z=265$ cm to 305 cm, plotted as a function of drift time after the beam pulse passes through the induction bunching module for the voltage waveform shown in Fig. 9. The beam energy is 322 keV, the energy spread, ΔE_b, is 190 eV, and $T_z=0.057$ eV.

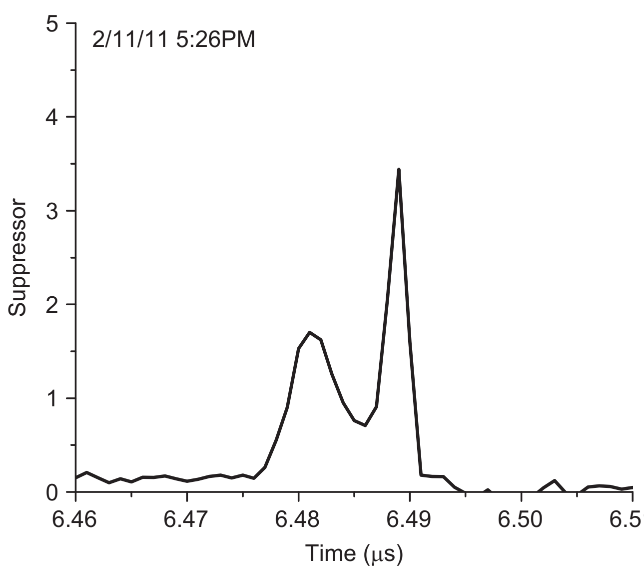

Fig. 13. Ion beam compression ratio profile in a pre-tuned shot from NDCX-I, as measured by a Fast Faraday Cup.

Fig. 14 compares simulated results with the results of the experiment. Fig. 14(a) compares the optimal compression ratio obtained from the analytical formulas with the optimal experimental results. Fig. 14(b) compares the optimal results from the experiment and the analytical formulas with the parameters, beam energy and target location, which were used in the experiment. The optimal results from the experiment more closely resemble the optimal results from the simulations. This is because the experiment is finely tuned in order to achieve the best results. To accurately analyze the data, the simulated beam energies were slightly varied to achieve the best results.

The results have also been simulated with the LSP particle-in-cell code [10] and showed good agreement with simulated compression ratio profiles obtained from the analytical formula in Eq. (10) (performed in Mathcad). The results of both simulations are identical, granted that both codes provide adequate resolution. As was observed with the Mathcad simulations, the results from the LSP PIC code simulations show that different parts of the beam compress over a wide range of target locations, as shown in Fig. 15. Fig. 16 compares the peak compression ratio

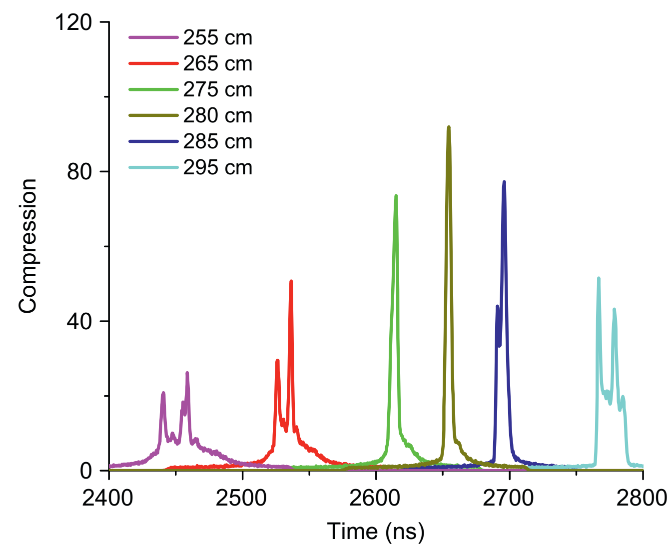

Fig. 15. Simulated compressed pulse waveform at six different target locations, from $z=255$ cm to 295 cm as a function of drift time after the beam pulse passes through the induction bunching module for the voltage waveform shown in Fig. 9. The beam energy is 317 keV, and the energy spread, ΔE_b, is 252 eV, where $T_{bz}=0.1$ eV.

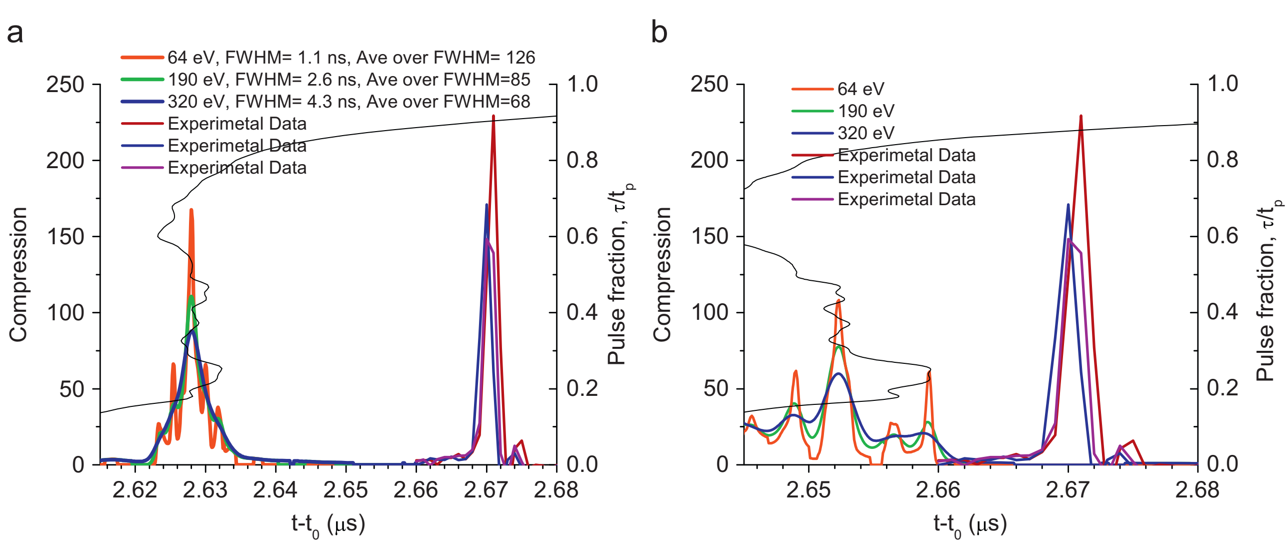

Fig. 14. Optimization of the simulated compressed pulse waveform for two beam energies at $z=2.846$ m: (a) $E_{b0}=316$ keV and (b) $E_{b0}=322$ keV, as a function of drift time, t–t_0, after the beam pulse passes through the induction bunching module for the voltage waveform shown in Fig. 9. This is shown together with the results for three different experimental shots.

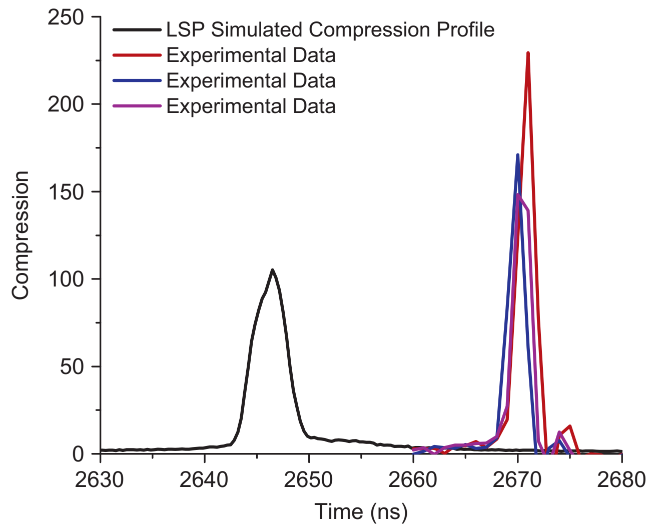

Fig. 16. LSP-simulated compression ratio profile compared with experimental results. For the LSP simulations, $z=2.79$ m, and $E_{b0}=317$ keV. The energy spread, ΔE_b, is 252 eV, corresponding to $T_{bz}=0.05$ eV.

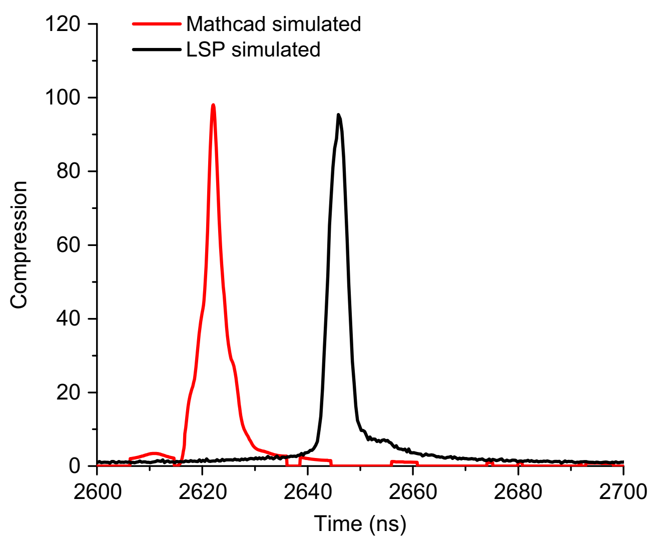

Fig. 17. Comparison of LSP simulations with Mathcad simulations. For Mathcad, $z=2.77$ m. For LSP, $z=2.79$ m. $E_{b0}=317$ keV. The energy spread, ΔE_b, is 252 eV, or $T_{bz}=0.1$ eV. The small difference in the focusing time, t_f, is associated with the finite gap effects of the NDCX-I induction bunching module [7]. This has the effect of shifting the applied velocity tilt profile to be slower than that estimated using the thin gap approximation.

profile obtained from the LSP simulations with the experimental results shown above. Fig. 17 compares the same LSP results with the peak compression ratio profile simulated by Mathcad using the same input parameters.

4. Conclusions

In this paper the NDCX-I experimental data for longitudinal compression of the beam pulse has been analyzed. A typical voltage pulse produced in the bunching module of NDCX-I is shown in Fig. 1, along with the voltage errors. A voltage pulse in the bunching module with amplitude of $\Delta U \approx 100$ kV results in the beam pulse compressing from $t_p=590$ ns down to $\delta t_p \approx 3.2$ ns during $t_f=2.8$ µs of the neutralized drift over 2.68 m. The voltage error, δU, is in the kV range. The errors in the applied voltage are much larger than the intrinsic energy spread, which is of order 100 eV, and they dominate the compression process.

For a 300 keV beam in NDCX-I, the spread in arrival time for the entire beam pulse at the target plane due to voltage errors and corresponding errors in the beam velocity, δv_b, is $\Delta t_p = t_f \Delta v_b / v_{b0} = t_f \Delta U / E_{b0} \sim 2.8\,\mu\text{s}/300 \approx 10\,\text{ns}$. However, at certain locations, a fraction of the beam is compressed more tightly if the voltage errors for this portion of the beam pulse are minimized. For example, for NDCX-I parameters, it was shown that the half-width of the compressed beam pulse can be reduced from 10 ns to 2 ns.

Improvements in NDCX-I voltage waveform reduce the voltage errors and allow a larger fraction of the beam pulse to compress, thereby increasing the compression ratio and reducing the compressed pulse width. However, because voltage errors are still large, different parts of the pulse compress over a range of times, causing the pulse to be compressed for many target locations. The beam energy can be optimized to reduce the errors of the applied voltage waveform and obtain one single peak at the target. This corresponds to the case when the applied voltage waveform can be approximated by an ideal voltage curve that compresses at the target plane with smaller voltage errors for a larger fraction of the beam pulse.

Acknowledgments

Research performed under the auspices of the US Department of Energy by the Princeton Plasma Physics Laboratory under Contract DE-AC02-76CH03073 and Lawrence Livermore National Laboratory under Contract DE-AC52-07NA27344.

References

[1] P. Sing Babu, A. Goswami, V.S. Pandit, Nuclear Instruments and Methods in Physics Research A 642 (2011) 1;
A.V. Eliseev, I.N. Meshkov, V.A. Mikhailov, A.O. Sidorin, Physics of Particles and Nuclei Letters 7 (2010) 473;
T.Kikuchi, K. Horioka, M. Nakajima, S. Kawata, Nuclear Instruments and Methods in Physics Research A 577 (2007) 103;
G. Franchetti, I. Hofmann, G. Rumolo, Physics Review Special Topics—Accelerators and Beams 3 (2000) 084201;
J.G. Wang, D.X. Wang, M. Reiser, Nuclear Instruments and Methods in Physics Research A 316 (1992) 112;
S. Humphries, Journal of Applied Physics 51 (1980) 2338.
[2] D.R. Welch, et al., Nuclear Instruments and Methods in Physics Research A 544 (2005) 236;
D.R. Welch, et al., Nuclear Instruments and Methods in Physics Research A 577 (2007) 231;
D.R. Welch, et al., Physics Review Special Topics—Accelerators and Beams 11 (2008) 064701.
[3] P.K. Roy, et al., Nuclear Instruments and Methods in Physics Research A 606 (2009) 22.
[4] I.D. Kaganovich, R.C. Davidson, M.A. Dorf, E.A. Startsev, A.B. Sefkow, E.P. Lee, A. Friedman, Physics of Plasmas 17 (2010) 056703;
Igor D. Kaganovich, Gennady Shvets, Edward Startsev, Ronald C. Davidson, Physics of Plasmas 8 (2001) 4180.
[5] R.C. Davidson, et al., Physics Review Special Topics—Accelerators and Beams 7 (2004) 104201.
[6] I.D. Kaganovich, et al., Effects of errors in velocity tilt on maximum longitudinal compression during neutralized drift compression of intense beam pulses: I. General descriptions.
[7] J.-L. Vay, P.A. Seidl, A. Friedman, Note on numerical study of the beam energy spread in NDCX-I, LBNL Report number LBNL-4288E, 2011 [Availaible online].
[8] J.E. Coleman, et al., Proceedings of the Particle Accelerator Conference, Albuquerque, NM, June 25–29, IEEE Catalog #07 CH37866, USA, 2007 ⟨http://accelconf.web.cern.ch/accelconf/p07/PAPERS/THPAS004.PDFS⟩, 2007, pp. 3516–3518.;
J.E. Coleman, Intense Ion Beams for Warm Dense Matter Physics, Ph.D. Thesis, University of California, Berkeley, 2008.
[9] P.K. Roy, et al., Physics Review Special Topics—Accelerators and Beams 9 (2006) 070402.
[10] A.B. Sefkow, et al., Physics of Plasmas 16 (2009) 056701;
A.B. Sefkow, R.C. Davidson, Physics Review Special Topics—Accelerators and Beams 10 (2007) 100101;
A.B. Sefkow, Ph.D. Thesis, Princeton University, 2007.

[11] P.K. Roy, et al., Physical Review Letters 95 (2005) 234801;
P. Seidl et al., Proceedings of the 2009 Particle Accelerator Conference, Vancouver, BC, Canada, TH3GAI04, 〈http://trshare.triumf.ca/~pac09proc/Proceedings/papers/th3gai04.pdf〉.
[12] P.A. Seidl, A. Anders, F.M. Bieniosek, J.J. Barnard, J. Calanog, A.X. Chen, R.H. Cohen, J.E. Coleman, M. Dorf, E.P. Gilson, D.P. Grote, J.Y. Jung, M. Leitner, S.M. Lidia, B.G. Logan, P. Ni, P.K. Roy, K. Van den Bogert, W.L. Waldron, D.R. Welch, Nuclear Instruments and Methods in Physics Research A A 606 (2009) 75–82.
[13] S.M. Lidia, P.K. Roy, P.A. Seidl, W.L. Waldron, E.P. Gilson, Commissioning results of the upgraded neutralized drift compression experiment, in: 2009 Proceedings of the Particle Accelerator Conference, Vancouver, BC, Canada, TU6PFP092, 〈http://trshare.triumf.ca/~pac09proc/Proceedings/papers/tu6pfp092.pdf〉.